IRANIAN JOURNAL OF CATALYSIS

A comparison between the heterogeneous photodecolorization of an azo dye using Ni/P zeolite and NiS/P zeolite catalysts

Alireza Nezamzadeh-Ejhieh*, Mahshid Khorsandi

Department of Chemistry, Shahreza Branch, Islamic Azad University, P.O. Box 311-86145, Shahreza, Isfahan, Iran,

Received 3 Sep 2010; received in revised form 3 Nov 2011; accepted 9 Nov 2011

ABSTRACT

A comparison of the photoefficiency of Ni(II) and NiS incorporated into zeolite P towards photodecolorization of Eriochrome Black T dye solution was investigated in a photocatalytic reactor using UV lamp as a light source. The effect of various experimental variables on the decolorization performance of the process was evaluated by examining catalyst dosage, temperature, initial dye concentration and pH of the dye solution. The obtained results showed better efficiency of NiS/P than Ni/P catalyst. The decolorization process in both case obeyed first-order kinetics.

Keywords*: Eriochrome Black T, NiS, Photodecolorization, Zeolite P, Heterogeneous catalysis*

1. Introduction

The synthetic azo dyes have considerable structural variety and are extremely stable under exposure to light and washing, and are also resistant to aerobic biodegradation by bacteria [1]. The toxicity and mass production of dyes leads to the necessity of treatment. There are several studies on the physical, chemical and biological treatment of dye containing effluents [2,3]. For the past few years "Advanced Oxidation Processes" (AOP) have become available. Among these processes, heterogeneous photocatalysis was found as an emerging destructive technology leading to the total mineralization of the most of organic pollutants [4]. The main advantage of use of AOP technique is that they transform the toxic organic pollutant into non-toxic products like CO_2 and H_2O [4].

Zeolites modified with transition metal ions have received increasing attention as promising catalysts for a variety of important reactions. Zeolites can serve as hosts to activate transition metal ions, offering a unique ligand system with multiple types of coordination for cations. In addition, the restricted pore size of zeolites could limit the growth or sintering of the nanoparticles of the cation even at high temperatures [5-7]. The aim of this paper was to investigate a comparison between the photoreactivity of the Ni-exchanged zeolite P and NiS/zeolite P as heterogeneous photocatalysts using UV source lamp for photodegradation of Eriochrome Black T dye. Effect of some key operating factors such as: temperature, pH, catalyst amount, initial dye concentration and effect of zeolite on the efficiency of the process were investigated.

* Corresponding author: E-mail: arnezamzadeh@iaush.ac.ir.
Tel: +98 321-3292515, Fax: +98 321-3211018

2. Experimental

2.1. Reagents

E.B.T ($C_{20}H_{12}N_3NaO_7S$) and all other chemicals with analytical grade were obtained from Merck. .deionized water was used throughout the experiments. The pH of solutions was appropriately adjusted with sodium hydroxide or hydrochloric acid solution as appropriate.

2.2. Synthesis of zeolite P and preparation of catalysts

Sodium silicate (acidimetric Na_2O 7.5-8.5%, acidimetric SiO_2 25.5-28.5%) and, aluminium chloride ($AlCl_3.6H_2O$) were used as silica and aluminium sources, respectively. Sodium hydroxide (NaOH) and water were used as mineralizing agent and solvent respectively. The NaOH solution (0.14 $g.mL^{-1}$) was added to aluminate solution (0.165 $g.mL^{-1}$) while the mixture was stirred and heated. Then the aluminate solution was added slowly into 14.53 g of sodium silicate in the polyethylene bottle and aged at room temperature with stirring for 4 h. Finally, the mixture at pH=13 was transferred to a reactor inside an oven with temperature of 100°C for 3 days. The solid product was filtered and washed with water until the pH of the filtrate dropped to 7. The products were dried at 100°C for 24 h. The obtained sample was zeolite P. For ion exchange experiments, 8 g of zeolite P powder was added to 100 mL of

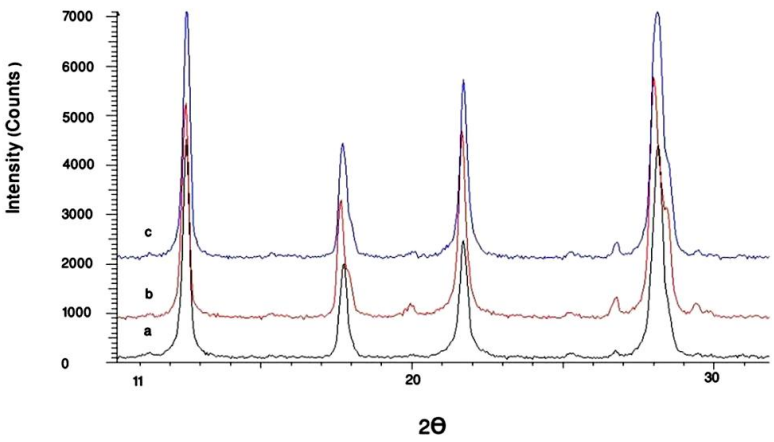

Fig. 1. X-ray diffraction pattern of parent synthesized zeolite P (a), Ni-P (b) and NiS-P (c) (in 2θ range of 11-32°)

0.1 M Ni^{2+} solution (as nitrate salt) and stirred at room temperature for 8 h. The procedure was repeated twice to complete ion exchange. The sample was filtered off, washed with water and dried at 110 ˚C. The color of the obtained sample (Ni-P) was greenish blue. Finally, sulfurizing of the Ni^{2+} ion was carried out with 0.1 M Na_2S solution. To make the reaction with S^{2-} ions, 2 g of Ni^{2+}-exchanged zeolite was added to 100 mL of 0.1 M solution of Na_2S at a fixed temperature and stirred for 30 min. The obtained sample was washed with water and collected by filtration to completely remove the sulfide ions. The obtained sample was fine powder with pale grey color. The sample was kept at ambient conditions and its color did not change during the time, indicating the high stability of the sample. To investigate the effect of nickel sulfide loading on decolorization process, three catalysts were prepared by ion exchange of zeolite P in 0.01, 0.1 and 0.2 M of Ni^{2+} solutions. Sulfurization of the samples was carried out according to above-mentioned method.

2.3. Characterization of samples

The X-ray diffraction patterns of zeolite P was prepared using a Bruker diffractometer (D8 Advance) with Ni-filtered copper radiation (Kα= 1.5406 Å) and 2θ range of 10-80□. FT-IR spectra of the samples, on KBr pellets were recorded with a Nicolet single beam FT-IR (Impact 400D) spectrometer in the range of 400-4000 cm^{-1} at room temperature. The surface morphology of samples was obtained using a Philips XL30 scanning electron microscope (SEM).

2.4. The catalytic activity

Photodecolorization experiments were performed with a photocatalytic reactor system. The bench-scale system is a cylindrical Pyrex-glass cell with 1.0 L capacity, 10 cm inside diameter and 15 cm height. Irradiation experiments were performed using medium pressure Hg lamp (75 W), then it was placed in a 5 cm diameter quartz tube with one end tightly sealed by a Tefloon stopper. The lamp and the tube were then immersed in the photoreactor cell with a light path of 3.0 cm. A magnetic stirrer was used continuously to guarantee good mixing of the solution. Unless otherwise stated, the reaction was carried out at room temperature under the conditions of 0.8 $g.L^{-1}$ of the solid catalyst in 50 mL solution of 20 ppm E.B.T dye, and the pH of the solution was initially 5. Generally, HCl (1M) and NaOH (1M) were used to adjust the pH value in the beginning of all experiments including the effect of pH study. The decolorization of E.B.T dye was analyzed by UV-Vis spectrophotometer (Carry 100 Scan). The decolorization was determined at the wavelength of maximum absorption (525 nm) of the dye. In the investigation of pH, due to shift in the λ_{max} value, new λ_{max} was determined by scanning the samples in range of 300-800 nm. Decolorization efficiency was determined using absorbance of solutions before and after photodecolorization experiments. The decolorization of E.B.T dye was fitted with first order kinetics [$\ln (C/C^o) = -kt$] (where C^o and C are the initial and final dye concentration at time t, respectively, and (k, min^{-1}), is the reaction rate constant). To determine the surface adsorption amount, control experiments in the dark condition were carried out in parallel in each case at the presence of catalyst on the decolorozation of E.B.T.

3. Results and Discussion

3.1. XRD patterns

The X-ray diffraction (XRD) patterns of zeolite P (ZP), Ni-P and NiS-P are shown in Fig. 1. The characteristic lines observed from XRD pattern in Fig. 1-a show a good agreement with the data of Na-P zeolite [8]. This analysis shows that the product has a typical zeolite P structure with no amorphous materials. Presence of the weak peaks in 2θ values of 20° and 26.8° in the Ni-P and NiS-P patterns (curve b and c in Fig 1), that no present in ZP pattern, can be show the incorporation of Ni^{2+} and Ni-S in the zeolite structure.

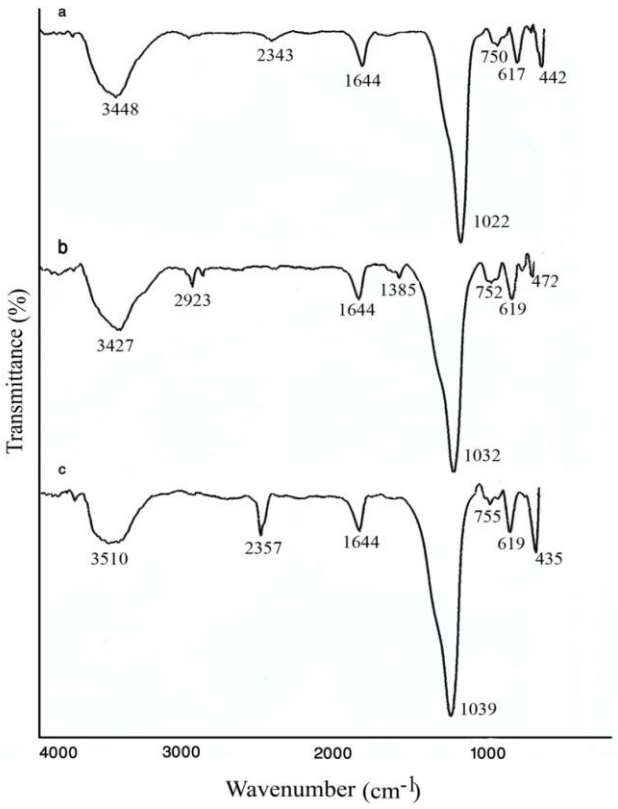

Fig. 2. FT-IR spectra of (a) Na-P (b) Ni-P and (c) NiS-P zeolites.

The powder XRD results of the ZP and the host-guest composite materials, Ni-P and NiS-P show similar diffraction peaks indicative of zeolite P. But, some differences, such as the broadening of the diffraction peaks, increasing or decreasing of some peaks intensity as well as the shift of the peak position to the slightly lower angles can be observed in the spectra. In fact, the intensities of the peaks in the host-guest composite materials are increased with respect to those of zeolite P. This increase of the peak intensities, can be related to the presence or incorporation of semiconductor inside the matrix structure.

3.2. FT-IR spectroscopy

FT-IR lattice vibration spectra were used to investigate the influence of nickel and nickel sulfide on the zeolite framework. Representative spectra of zeolite P, Ni-P and NiS-P in the range of 450-4000 cm^{-1} are shown in Fig. 2. According to the Fig. 2-a, the observed frequencies agree with the infrared spectral data, which has been obtained for zeolite P by Flanigen *et al.* [9]. Infrared spectroscopy can reflect the changes of the frameworks configuration of the zeolite host after the incorporation of the guests. Changes of the characteristic bands took place between the host zeolite P and the host-guest materials Ni-P and NiS-P. The greenish blue color after ion exchange with Ni^{2+} ions is the primary evidence for incorporation of Ni^{2+} into zeolite framework. In addition, in NiS-P spectral changes around 755 cm^{-1} are different from other spectra. These results demonstrated that the guest NiS incorporated into the zeolite P had some interactions with the inner surfaces of zeolite P host at the same time. The product after the precipitation process shows a change in color from greenish blue to pale gray that in turn can be shows conversion of Ni^{2+} to NiS in the zeolite.

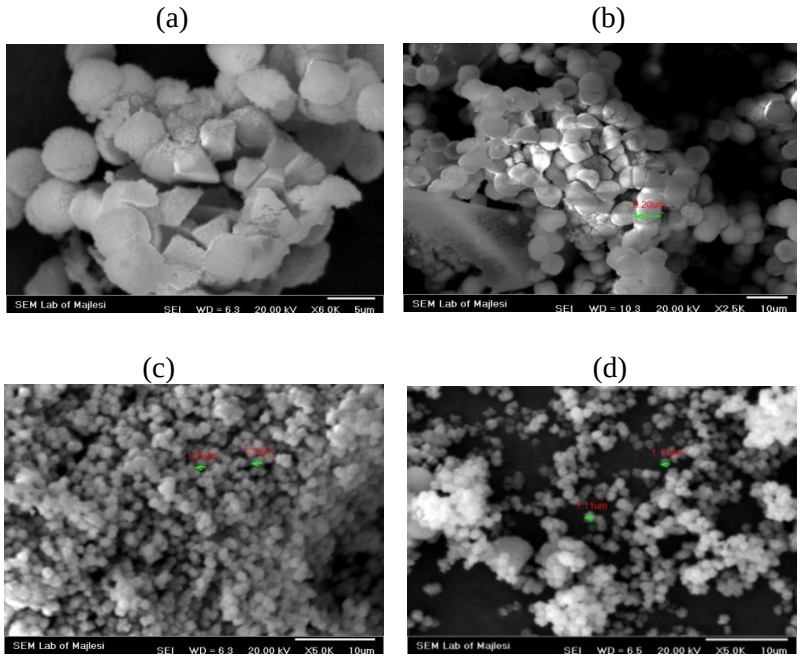

Fig. 3. SEM images of zeolite P (a,b), Ni-P (c) and NiS-P (d).

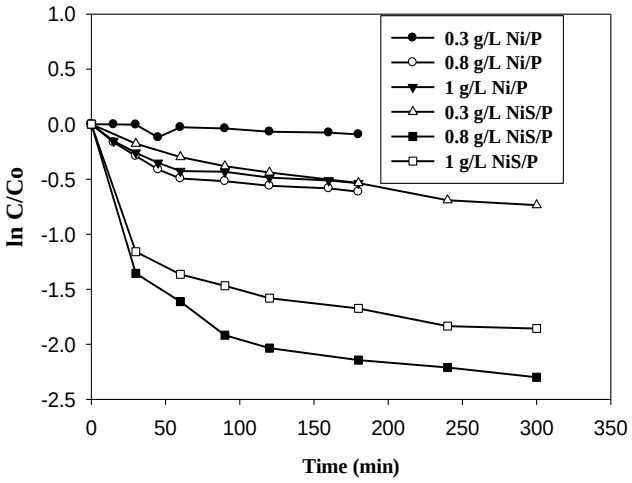

Fig. 4. Effect of catalysts dosage on the decolorization efficiency; initial dye concentration, 20 ppm; initial pH,

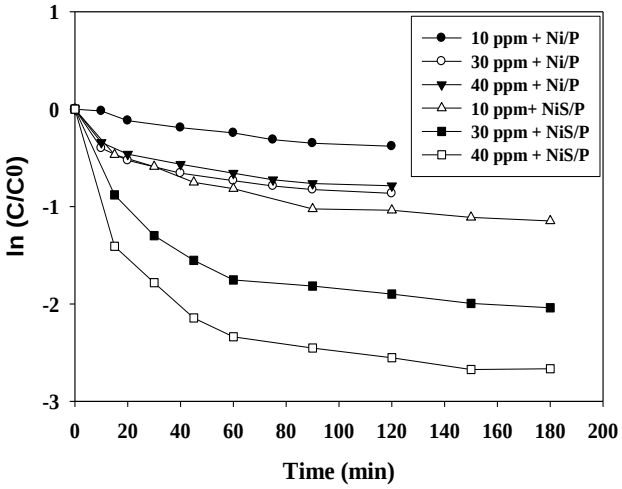

Fig. 5. Effect of the initial dye concentration on decolorization efficiency; 0.8 $g.L^{-1}$ of catalyst; initial solution pH, 5.

3.3. SEM analysis

The surface morphology of zeolite P (a,b), Ni-P (c) and NiS-P (d) was studied by scanning electron microscopy and the SEM pictures are presented in Fig. 3. The crystallites of the unloaded zeolite, with size about 1.75 µm, have a very well defined spherical grain like crystals. The image of the loaded samples also shows the spherical crystals that indicate the zeolite crystallites are not affected by the NiS loading. The average particles size of Ni-P and NiS-P samples is about 1.60 and 1.23 µm, respectively. The image of loaded samples shows that spherical grain like of zeolite crystals is not affected by the NiS and Ni^{2+} loading.

3.4. Catalytic activity of Ni/P zeolite sample

3.4.1. Effect of dosage of Ni/P and NiS/P catalysts

As the catalyst dose is one of the major kinetic factors of photodegradation, some experiments were carried out by varying the amount of catalysts and the obtained results are presented in Fig. 4. For both catalysts, the decolorization of E.B.T dye was fitted with first order kinetics [ln (C/C°) = -kt] (where C° and C are the initial and final dye concentration at time t, respectively, and (k, min^{-1}), is the reaction rate constant). On the other hand, increasing in the slop of the curves shows increase in the decolorization efficiency. As the concentration range increases from 0.1 to 0.8 $g.L^{-1}$, the number of absorbed photons increased owing to an increase in the number of catalyst particles. The density of particles in the rate of illumination also increases and so the rate is enhanced. The observed enhancement in decolorization is probably due to an increased number of available absorption and catalytic sites on the catalyst [10]. As seen the rate of the reaction (the slopes of the curves) increases with increasing catalyst dosage up to 0.8 $g.L^{-1}$, while at higher concentrations degradation is adversely affected. The latter is believed to be due to (i) a screening effect of excess catalyst particles, thus masking part of the photo sensitive surface and consequently hindering light penetration, and (ii) increased light reflectance onto the catalyst surface both of which occur at increased catalyst concentrations [11,12].

3.4.2. Effect of initial dye concentration

The effect of initial dye concentration ranging from 10 to 50 ppm on photodecolorization of EBT dye by photocatalysts was investigated under UV irradiation. The obtained results as a function of the initial dye concentration on the kinetics of the EBT photodecolorization efficiency are presented in Fig. 5. The lifetime of hydroxyl radicals is only a few nanoseconds and hence they can only react where they are formed. Increasing the quantity of EBT molecules per volume unit logically enhances the probability of collision between organic matter and oxidizing species leading to an increase in the photodecolorization [13]. It can be seen that the photodecolorization efficiency of dye decreased with increasing initial concentration of dye from optimum values. One possible cause for such results is the UV radiation-screening effect of the dye itself. At a high dye concentration, a significant amount of UV radiation may be absorbed by the dye molecules rather than the catalyst particles. Consequently, by increasing the initial dye concentration, the photon flow reaching the catalyst particles decreased due to the fact that increasing numbers of photons were absorbed by the dye molecules present in the solution and/or on the catalyst surface thus reducing the efficiency of the catalytic reaction [14]. Another possible cause is the interference from intermediates formed upon UV photocatalytic of the parental dye. These intermediates may include aromatics, aldehydes, ketones and organic acids as shown by previous studies with various aromatic compounds [15-17]. They may compete with the dye molecules for the limited adsorption and catalytic sites on the catalyst particles and thus inhibit decolorization.

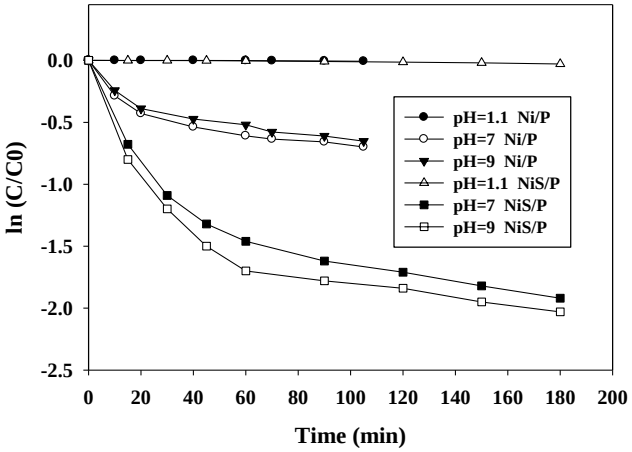

Fig. 6. Influence of solution pH on the E.B.T. dye decolorization; 0.8 $g.L^{-1}$ of catalyst; initial dye concentration, 20 ppm.

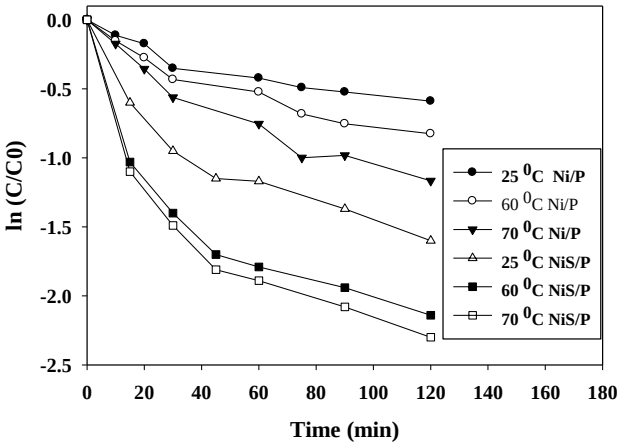

Fig. 7. Effect of the reaction temperature on photodecolorization efficiency; 0.8 $g.L^{-1}$ of catalyst; initial solution pH, 5; initial dye concentration, 20 ppm.

4.3. Influence of pH on the decolorization of EBT

The most important parameter that influences the photocatalytic degradation is solution pH [10]. The effect of pH in the range of 1-11 on the kinetics of the decolorization of EBT versus time is presented in Fig. 6. As mentioned in the literature [13] ·OH can be formed by the reaction between hydroxide ion and positive hole. So, an alkaline condition would thus favor ·OH formation and enhance degradation [15,18,19]. In alkaline solutions, interaction between catalyst surface ($Si\text{-}O^{-}$) and dye (specifically the nitrogen group) favors the adsorption of the dye on the surface and accordingly the photocatalytic activity increases. As mentioned in the literature [13], in the initial acidic pHs, concomitant with acidification of the solution by HCl produces a high amount of conjugated base in the solution. The anion Cl^{-} is able to react with hydroxyl radicals leading to inorganic radical ions ($ClO^{\cdot}$). This inorganic radical anion shows a much lower reactivity than ·OH, so that it does not take part in the dye decolorization. There is also a drastic competition between the dye and anions with respect to ·OH. Hence, with increasing pH an increase in decolorization efficiency is observed. As the results show, there is a decrease in removal efficiency at pH higher than the optimum value. Authors suggest that at high concentration of $^{-}$OH two processes may take place leading to the deactivation of ·OH. First, the $H_2O^{\cdot}_2$ and $HO^{\cdot}_2$ radicals were formed due to the reaction of ·OH with $^{\cdot}$OH. The reactivity of these radicals with organic dye is very low compared to that of ·OH [13]. Second, due to the presence of high amounts of ·OH radicals, the radical-radical reactions takes place at higher pH values.

3.4.4. Effect of the reaction temperature

The influence of temperature on the dye removal using 20 ppm dye concentration, pH 5, 0.8 $g.L^{-1}$ catalysts was performed at 25, 60, 70, 80 °C. The photodecolorization efficiency was increased by increasing the temperature (Fig. 7). Because the reaction activity of $OH^{\bullet}$ radical increases with the increase of temperature which favors the photodecolorization of dye [20]. The rise in the temperature showed that it was effective at the initial stages of the process. It has reported that an increase in temperature helps the reaction to compete more effectively with e^{-}_{CB} - h^{+}_{VB} recombination [21]. On the other hand, an increase in temperature decreases the solubility of oxygen in water which is not desirable. Temperature higher than 50 °C not recommended because of significant evaporation of the solution during the experiments at higher temperatures.

4. Conclusions

The results of this research demonstrated that both Ni/P and NiS/P zeolites are affecting catalysts on the photodecolororization of EBT dye. In our idea, in the Ni/P catalyst bonding of Ni(II) cations with oxygen atoms of the zeolite framework yield a semi NiO semiconductor in the zeolite structure. This comparison showed that the reactivity of the NiS/P is higher than Ni/P catalyst which shows the better photoreactivity of NiS with respect to the NiO.

References

[1] C-C. Hsueh, B-Y. Chen, J. Hazard. Mater. 141 (2007) 842-849.
[2] T. Robinson, G. McMullan, R. Marchant and P. Nigma, Bioresource Technol.,77 (2001) 247-255.
[3] G. Sivalingam, K. Nagaveni, M.S. Hegda and G. Madras, Appl. Catal. B: Environ. 45 (2003) 23-38.
[4] A. Nezamzadeh-Ejhieh, Sh. Hushmandrad, Appl. Catal. A: Gen. 388 (2010) 149–159.
[5] A. Nezamzadeh-Ejhieh, S. Moeinirad, Desalination 273 (2011) 248–257.

[6] Z.M. El-Bahy, M.M. Mohamed, F.I. Zidan, M.S. Thabet, J. Hazard. Mater. 153 (2008) 364-371.
[7] A. Nezamzadeh-Ejhieh, Z. Salimi, Appl. Catal. A: Gen. 390 (2010) 110–118.
[8] H. Faghihian, M. Kamali, Int. J. Environ. Pollut. 19 (6) (2003), 557-566.
[9] E.M. Flanigen, H. Khatami, H.A. Szymanski, Molecular Sieve Zeolites, Adv. Chem. Ser. 101, American Chemical Society, Washington, D.C., (1971) p 201.
[10] M.Y. Ghaly, J.Y. Farah, A.M. Fathy, . Desalination 217 (2007) 47-84.
[11] C. Fotiadis, N.P. Xekoukoulotakis, D. Mantzavions, Catal. Today 124 (2007) 247-253.
[12] B. Damardji, H. Khlaf, L. Duclaux, B. David, Appl. Clay Sci. 45 (2009) 98-104.
[13] M.B. Kasiri, H.Aleboyeh, A. Aleboyeh, Appl. Catal. B: Environ. 84 (2008) 9-15.
[14] A. Mills, R.H. Davis and D. Worsley, Chem. Soc. Rev. 22 (1993) 417–434.
[15] N. Serpone, R. Terzian, C. Minero and E. Pelizzetti, American Chemical Society, New York, 1993, pp. 281–314.
[16] O. d'Hennezel, P. Pichat and D.F. Ollis, A: Chem. 118 (1998) 197–204.
[17] K. Tanaka, K. Padermpole and T. Hisanaga, Water Res. 34 (2000) 327–333.
[18] H.R. Pouretedal, A. Norozi, M.H. Keshavarz, A. Semnani, J. Hazard. Mater. 162 (2009) 674-681.
[19] J. Saien, A.R. Soleymani, J. Hazard. Mater. 144 (2007) 506–512.
[20] J. Chen, L. Zhu, Catal. Today 126 (2007) 463-470.
[21] J. Saien, S. Khezrianjoo, J. Hazard. Mater. 157 (2008) 269-276.